Iris Recognition Based on Directional Empirical Mode Decomposition

Wei-Yu Han[1], Yen-Po Lee[1], Jen-Chun Lee[2], and Chien-Ping Chang[1*]

[1] Department of Computer Science and Information Engineering, Ching Yun University
[2] Department of Electrical Engineering, Chinese Naval Academy, Taiwan

ABSTRACT

As the increasing demand of information security with entrance governing of military building, so does the attention pay the biometrics based, automated person identification. Among current biometrics approaches, one of the most promising techniques is the basis on the human iris. In this paper, we proposed an effective algorithm for iris recognition. The methodology involves an extraction of iris features using directional empirical mode decomposition (DEMD) and fractal dimension. After the preprocessing procedure, the normalized effective iris image is decomposed into different 2D intrinsic mode function (IMF) components according to different frequency by the directional empirical mode decomposition. Then, the texture feature of each intrinsic mode function image is obtained via the differential box-counting method. The experiment results on the CASIA and ICE iris databases show that the presented schema achieves promising performance and is feasible for iris recognition.

Keywords: Biometrics, directional empirical mode decomposition, intrinsic mode function, fractal dimension

運用方向性經驗模態分解法於虹膜識別

韓維愈[1]　李衍博[1]　李仁軍[2]　張劍平[1*]

[1] 清雲科技大學電腦科學與資訊工程學系
[2] 海軍軍官學校電機工程學系

摘　　要

隨著資訊安全與門禁管制的需求逐漸增加，越來越多的個人身分認證傾向於運用生物識別；在現階段生物識別方法中，人類虹膜仍是最有效的方法之一。本文提出運用方向經驗模態分解(directional empirical mode decomposition, DEMD)及碎形維度(fractal dimension, FD)方法，有效擷取虹膜特徵實施識別。首先將正規化後之虹膜影像，運用方向經驗模態分解法依據不同頻率分解為數張二維本質模態函數(2D intrinsic mode function , IMF)影像，接著運用差方盒計算方法，在數張本質模態函數影像中找出虹膜紋理特徵。為評估方法之有效性，本文運用三種相似度測量法分別實施識別；實驗驗證於兩種公認的資料庫(CASIA 及 ICE)，結果顯示出提出的演算法具有較佳的效果。

關鍵字：生物認證，方向經驗模態分解，本質模態函數、碎形維度

文稿收件日期 100.6.14; 文稿修正後接受日期 101.3.1 ; *通訊作者
Manuscript received June 14, 2011; revised March 1, 2012. ; *Corresponding author

1. I. INTRODUCTION

Biometrics deals with the uniqueness of an individual arising from their physiological or behavioral characteristics for the purpose of personal identification. Biometric recognition [1] systems verify a person's identity by analyzing his/her physical features or behavior (e.g. face [2], fingerprints, palm prints, retina, handwriting signature, and gait). Therefore, it is more convenient and securer than the traditional authentication methods. Among all the biometrics authentication methods, a lower error recognition rate achieved by iris recognition has been reported [1, 3] and received increasing attention in recent years. Physiological characteristics of human's eyes consist of sclera, iris, and pupil, and their boundaries are like circles with varied radii. Iris is a nearly annular colored portion between the black pupil and white sclera, and it is embedded with tiny muscles that affect the pupil size and occupy most areas in the eye. It appears that the phenotypic random patterns are visible in the human iris constituted by lots of irregular blobs, such as freckles, coronas, stripes, furrows and crypts [4]. Such iris pattern is a unique, stable, and non-invasive biometric feature suitable for individual verification.

Daugman first introduced a successful algorithm for iris recognition [5]. His algorithm is accurate and efficient. Large scale tests have been conducted and the results show that his system can achieve almost zero error rate [5-9]. After [1], the related researches on iris recognition have been closely investigated. In general, an iris recognition system usually comprises the following four main steps: iris image quality assessment, iris image preprocessing, feature extraction, and feature matching. Iris image quality also plays an essential role at the recognition performance for an effective algorithm of iris recognition, because poor quality images can significantly degrade the performance of iris recognition systems. The goal of assessment of an eye image is to acquire a high quality image to support iris recognition. Then, iris region segmentation is performed to localize the inner and outer boundary of the iris area by an image processing algorithm. Additionally, the areas obscured by specular reflections, eyelids, eyelashes, and so on, should be detected and discarded to improve the performance of recognition. Next, the Gabor or wavelet transform is typically used to extract the iris features. Finally, a decision step is used to compare the extracted features with those in the database for identifying who the user is. The main difficulty of iris recognition comes from the fact that it is not easy and fast to extract unique features in an efficient way. Furthermore, feature comparison and classification processes suitable for iris patterns are required to reach high accuracy. These problems have been identified by several researchers [5-28]. Therefore, how to design a robust method for iris recognition becomes a nontrivial and challenging issue. In our works, during the feature extraction process, we employ the directional empirical mode decomposition (DEMD) to analysis iris image, the idea is to decompose the iris image into its 2D intrinsic mode functions (IMFs), of which fractal dimension is calculated as a feature vector.

Empirical mode decomposition (EMD) is the key part of the hilbert huang transformation (HHT), which proposed by Huang in 1998 [12]. Contrary to almost all the previous methods, this new method is intuitive, direct and adaptive, with the basis of the decomposition based on and derived from the data. It has been widely employed in earthquake motion, financial series analysis et al. [13, 14], and the directional empirical mode decomposition (DEMD) is modified by Liu et al. and be employed in texture segmentation [15]. This paper proposes a novel algorithm for automatic iris recognition system based on DEMD and fractal dimension are presented. The DEMD is applied to extract the multiple scale features at different resolutions from the iris image. Fractal dimensions obtained from multiple scale features are completely used to characterize the iris textures. The different similarity measures are used to recognize the given iris image from the iris database.

This work is organized as follows. Section 2 briefly summarizes related works. A detailed description of the proposed method for iris recognition is given in Sec. 3. Experimental

results are demonstrated and discussed in Sec. 4, before conclusions in Sec. 5.

2. II. RELATED WORKS

In the process of the iris recognition, it is essential to convert an acquired iris image into a suitable code that can be easily manipulated. Thus, we will take a brief look at the process of feature extraction and representation from the recent remarkable works. Existing iris recognition systems were developed using several approaches. Major differences among the systems are methods used in analyzing and extracting iris features. Examples of those systems can be roughly divided into four main categories: phase-based approaches [5-9], zero-crossing representation [16-18], texture analysis [19-24], and intensity variation analysis [10, 25]. Daugman's algorithm [5] adopted the 2D Gabor filters for feature extraction to demodulate the iris phase information. Each phase structure was quantized into one of four quadrants in the complex plane. The Hamming distance was further used to calculate the distance between iris codes of 2048 bits. In the past decade, Daugman had constantly modified and improved his recognition algorithms. Based on active contours, a recent paper [7] presented alternative segmentation methods to transform an off-angle iris image into a more frontal view. Moreover, a description of new score normalization scheme was used for computing the Hamming distance that would be accounted for the total amount of unmasked data available in the comparison. Boles and Boashash [16] presented the zero crossing of a one-dimensional wavelet transform to represent distinct levels of a concentric circle for an iris image, and two dissimilarity functions were used for matching the obtained iris features. To extend the approach of Boles and Boashash, Sanchez-Avila & Sanchez-Rellio [17] further proposed using different distance measures for feature matching. Furthermore, Monro *et al.* [18] used the discreet cosines transform (DCT) for feature extraction. They applied the DCT to overlap rectangular image patches rotated 45° from the radial axis. The differences between the DCT coefficients of adjacent patch vectors are then calculated, and a binary code is generated from their zero crossings. To increase the speed of the matching, the three most discriminating binarized DCT coefficients are kept, and the remaining coefficients discarded.

Regarding texture analysis schemes, Wildes *et al.* [19] used the Laplacian pyramids to analyze the iris texture and combine the features from e. Then, normalized correlation was selected to decide whether the input image and the enrolled image belong to the same class. Lim et al. [20] decomposed an iris image into four levels with different frequency components using 2-D Haar wavelet transform, and the fourth level with high frequency information was quantified to form an 87-bit code. Then, a modified competitive learning neural network was used for classification. Ma et al. [21] proposed a well-known texture analysis method (multichannel Gabor filtering) to capture both global and local details from an iris image. Recently, Tisse et al. [22] constructed the analytic image (a combination of the original image and its Hilbert transform) to demodulate the iris texture. Lee et al. [23] proposed a new model of texture analysis to extract local edge patterns (LEPs) (e.g., high frequency parts) from the iris texture as features for iris recognition. Chang et al. [24] used the 1-D empirical mode decomposition (EMD) as a low-pass filter and extracted the iris features for accurate iris recognition. Ma et al. proposed a local intensity variation analysis-based method and adopted the Gaussian-Hermite moments [10] and dyadic wavelet [25] to characterize the iris image for recognition. Additionally, Noh et al. [26] used independent component analysis (ICA) methods to reduce the size of the iris feature without sacrificing the recognition accuracy. Proença et al. [27] proposed a new iris classification strategy by dividing the normalized iris image into six regions and extracted the feature of each region independently.

All iris recognition algorithms are based on statistical classifiers and local image features, which are noises sensitive and have difficulties delivering the perfect recognition performance. In other words, feature extraction is a crucial processing stage for iris recognition. Traditionally, basis decomposition techniques, such as Fourier decomposition or wavelet decomposition, are selected to analysis real

world signals [28]. Also, Fourier and wavelet descriptors have long been used as powerful tools for feature extraction [29-31]. However, the main drawback of these approaches is that the basis functions are fixed and do not necessarily match the varying nature of the signals. On the other hand, the method of EMD can be decomposed any complicated signal into a finite and often small number of IMF components that are used as a set of basis functions to represent the signals. Those extracted IMF components can match the signal itself very well. In [24], we adopt and modify the 1D EMD technique to extract residual components as features from iris images for recognition. Experimental results show that the 1D EMD is suitable for feature extraction, but it is not to employ the 2D correlation of the iris image. Liu et al. [15] developed an algorithm based on directional empirical mode decomposition (DEMD) to extract features at multiple scales or spatial frequencies. This method, derived from the image data and fully unsupervised, permits to analyze nonlinear and non-stationary data as texture images. In this paper, DEMD method is applied to decompose iris image into its 2D intrinsic mode functions (IMFs) image. It has been proven to be a good tool to decompose and extract image features, mainly because it takes into account the spatial correlation between traces, which does not occur with other methods that make the filtering only in one direction (time), like the 1D EMD and WT.

The concept of the fractal was first introduced by Mandelbrot [32], who used it as an indicator of surface roughness. Fractal dimension extracts roughness information from images considering all available scales at once. Single scale features may not be sufficient to characterize the textures, thus multiple scale features are considered necessary for a more completely textural representation [33]. Several algorithms have been proposed to estimate the fractal dimension of a 2-D image such as [34-36]. The fractal dimension can be used to analyze the texture of iris images effectively [37, 38]. In our experiments, we find that the 2D IMFs decomposed images can provide adequate texture information for different frequency bands which can be effectively represented by the fractal dimension to offer a good performance.

III. PROPOSEDMETHOD FOR IRIS RECOGNITION

In this work, an iris recognition algorithm

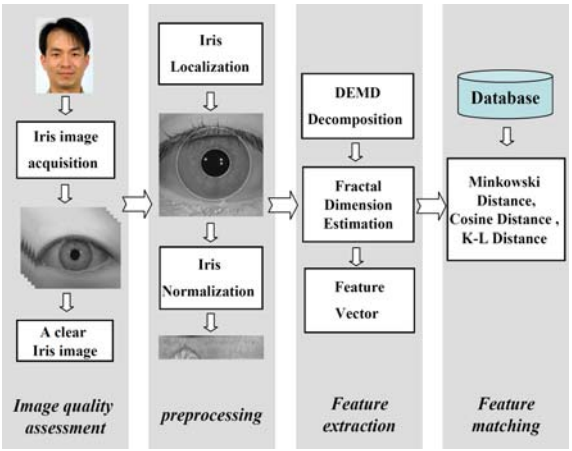

Fig. 1. Block diagram of the proposed iris recognition system.

is presented, which includes four basic processes: image quality assessment, preprocessing, feature extraction, and matching. Figure 1 shows how the proposed algorithm works. Detailed descriptions of these four steps are introduced in the following sections.

3.1 Image Quality Assessment

When capturing iris images, one usually obtains a sequence of images rather than a single image. However, not all the iris images in the input sequence are high quality and suitable for recognition. After observing the unsuitable iris images in [23], we found that the low quality iris images can be roughly categorized into two classes, namely, blurred images caused by defocused or motion, and occluded images severely affected by eyelids or eyelashes (an example is shown in Fig. 2). In [39], we proposed a method that evaluates the quality of iris images automatically to discard the unsuitable images. First, the texture information about the iris regions adjoining the pupil on the right and left sides (64×64) are calculated to distinguish the blurred images from the clear images. Next, the valid iris regions are employed

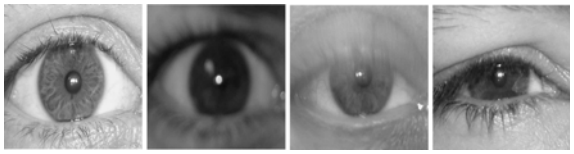

(a) (b) (c) (d)

Fig. 2. Differences between a high and low quality iris images. (a) A clear image. (b) A defocused image. (c) A motion blurred image. (d) An occluded image.

to discriminate between the occluded images and useful images. Finally, the statistic's method is employed to select the high quality iris images. The iris image quality assessment procedures utilized in this paper had been clearly described in our previous work [39]. Based on Eq. (1), we can assess the quality of an image and select the high quality iris images.

$$Q = (Q_1 \,\&\, Q_2), \tag{1}$$

$$Q_1 = \begin{cases} 0, & q_1 < C_{lowq_1} \\ 1, & q_1 \geq C_{lowq_1} \end{cases}, \text{and } Q_2 = \begin{cases} 0, & q_2 < C_{lowq_2} \\ 1, & q_2 \geq C_{lowq_2} \end{cases}$$

where q_1 and q_2 are the quality descriptors of the in focus image and the useful (un-occluded) image, respectively; C_{lowq_1} and C_{lowq_2} are the confidence intervals for the quality descriptors (q_1 and q_2), respectively; & denotes the logical AND operation.

3.2 Image Preprocessing

To ensure that the proper iris features can be extracted from the eye image, it is essential to perform preprocessing on the eye images. The image preprocessing procedure to extract the iris from the eye image is operated by three steps. The first is to locate the iris area. Then, the located iris is normalized and converted to a rectangular window of a fixed size to achieve the approximate scale invariance. Finally, the most irrelevant parts (such as eyelid, pupil, and eyelashes) are removed from the normalized image much by selecting an appropriate region of interest (ROI).

The preprocessing procedure utilized in this work is well described in [23], which uses only a triad of points for locating the inner and outer boundaries of the iris based on Thales's theorem. The normalization process involves unwrapping the iris and converting it into its equivalent polar coordinates. We transform the circular iris area into a block by using Daugman's rubber sheet model [5, 6]. The pupil center is considered as the reference point and a remapping formula is used to convert the points from the Cartesian scale to the polar scale. In our experiments, the radial resolution and the angular resolution are set to 64 and 512 pixels, respectively. Fig. 3 illustrates the results of the preprocessing process for the iris image.

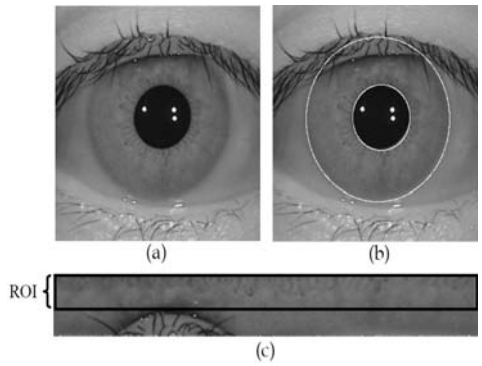

Fig. 3. The results of iris image preprocessing (a) the original iris image, (b) the image with the located iris area, and (c) the ROI from the normalized iris image.

3.3 Feature Extraction

Despite all normalized iris templates having the same size, there would be eyelashes and eyelids on the templates, and those bring the performance down on iris recognition. Therefore, the ROI is selected to remove the influence of eyelashes and eyelids, which is shown in Fig. 3(c). The features are extracted only from the upper half region (32×512) close to the pupil that can provide most of the discriminating information [40]. These processes can eliminate most of the interference and produce more precise iris templates for feature extraction.

3.3.1 1-D Empirical Mode Decomposition

Empirical Mode Decomposition (EMD) was first introduced by [12] and provides a powerful tool for adaptive multiscale analysis of non-stationary signals. As far as the one-dimensional (1-D) case is concerned, studies were carried out to show the similarities of EMD with the selective filter bank decomposition [41]. Its efficiency for signal de-noising was also shown in [42]. The EMD is completely posterior in regard to the

decomposition of the data into intrinsic mode functions (IMFs) and does not assume anything about the data, contrary to Fourier methods where data is assumed linear and stationary. Because of the adaptive nature of EMD, it has been numerically shown a means to better describe temporal patterns in non-stationary nonlinear time series than traditional methods such as Wavelet and Fourier methods. These interesting aspects of the EMD motivate us to extend it to iris recognition [24].

The basis of EMD is the construction of some IMFs that are formed through a so-called "sifting" process (SP). The principle is to locally identify the most rapid oscillations in the signal, defined as a waveform interpolating interwoven local maxima and minima. To do so, the local maxima points and the local minima points are interpolated with a cubic spline for determining the upper and the lower envelope, respectively. The mean envelope, and the half of sum of the upper and the lower envelopes are then subtracted from the original signal, and the same interpolation scheme is iterated on the remaining signal. The "sifting" process terminates when the mean envelope is reasonably zero everywhere, and the resultant signal is designated as an IMF. The highest order IMF is iteratively extracted by applying the procedure for the original signal, and the successive higher order IMF are iteratively extracted by applying the same procedure after removing the previous IMFs. An IMF is characterized by some specific properties which (a) in the whole data set, the number of extrema and the number of zero-crossings must either be equal or differ from most by 1, and (b) at any point, the mean value of the upper and the lower envelopes is equal to zero. Hence, for a given signal, EMD ends up with a representation of the form:

$$S = \sum_{j=1}^{n} I_j + r \tag{2}$$

where I_j is the jth mode (or IMF) of the signal, and r is the residual trend. The sifting procedure generates a finite (and limited) number of IMFs that are nearly orthogonal to each other.

3.3.2 Directional Empirical Mode Decomposition

The DEMD method is an adaptive and data-driven technique that decomposes an image into a small set of sub-images called 2D IMFs, representing the high and low frequency components of the original image and a residue. Similar to the definition for 1DIMF and EMD, 2D IMF and DEMD are defined as following:

Definition 1: Given $\theta \in [0, \pi)$, signal $u(x,y)$ is defined as 2D IMF corresponding to θ if for $\forall c$, it satisfies the following condition:

$$v_{1,c}^{\theta} = \begin{cases} u(x, \tan\theta \cdot x + c), & 0 \le \theta < \pi, \theta \ne \pi/2 \\ u(x, \cdot), & \theta = 0. \end{cases} \tag{3}$$

$$v_{2,c}^{\theta} = \begin{cases} u(x, \tan(\theta + \pi/2) \cdot x + c), & 0 \le \theta < \pi, \theta \ne \pi/2 \\ u(\cdot, x), & \theta = \pi/2. \end{cases}$$

then both of $v_{1,c}^{\theta}$ and $v_{2,c}^{\theta}$ meet the condition $(*)$. $v_{1,c}^{\theta}$ and $v_{2,c}^{\theta}$ are called the IMF.

Definition 2: DEMD of 2D image $I(x,y)$ for direction θ is defined as the decomposition:

$$I(x,y) = \sum_{i=1}^{N} imf_i^{\theta}(x,y) + r_N^{\theta}(x,y) \tag{4}$$

where $imf_i^{\theta}(x,y)$ are 2D IMFs for θ and $r_N^{\theta}(x,y)$ has at least one monotonic 1D sampling for $v_{1,c}^{\theta}(x)$ or $v_{2,c}^{\theta}(x)$.

The sifting process to find the 2D IMFs of an image $I(x,y)$ comprises the following steps:

Step1: Initialize: $r_0(x,y) = I(x,y), \quad i = 1.$

Step2: Extract the i^{th} IMF of $imf_i(x,y)$:

(1)Initialize: $r_{i-1}(x,y) = I^{\theta}(x,y)$ $(i = 1)$, where $I^{\theta}(x,y)$ is the rotated form of $I(x,y)$ by clockwise rotating θ.

(2)Get the middle envelops of $h_{j-1}(x,y)$

1. Attract the local maximums of each row. Then interpolate the maxima and minima by bi-cubic method to get the upper and lower envelopes of each row. Composite the 1D envelopes to 2D envelope: $h_{midupper}(x,y)$ and $h_{middown}(x,y)$.
2. So we get the middle envelope as $m_{mid}(x,y) = (h_{midupper}(x,y) + h_{middown}(x,y))/2;$
3. Get the middle envelop $m_{j-1}(x,y)$ of $m_{mid}(x,y)$ for each column.

(3) $h_j(x,y) = h_{j-1}(x,y) - m_{j-1}(x,y)$;

(4) Once the stop criterion

($SD = \sum_{x=0}^{X}\sum_{y=0}^{Y}[\frac{|h_{1(k-1)}(x,y) - h_{1k}(x,y)|^2}{h_{1(k-1)}^2(x,y)}] < r$), (r is constant) is satisfied or SD starts to increase, let $imf_i(x,y) = h_j(x,y)$. Otherwise go to (2). In addition let $j = j+1$.

Step3: $r_i(x,y) = r_{i-1}(x,y) - imf_i(x,y)$.

Step4: If there exists monotonic 1D sampling of $r_i(x,y)$ for row or column, the process is ended. Otherwise let $i = i+1$ and turn to step2.

Step5: Rotate imf_j, $j = 1,...,N(N=i)$ and $r_N(x,y)$ anticlockwise by θ to compute imf_j^θ, $j = 1,...,N(N=i)$ and $r_N^\theta(x,y)$.

Thus arbitrary 2D signal $I(x,y)$ can be decomposed into the form (4). where imf_j^θ is the jth 2D IMF component and $r_N^\theta(x,y)$ is the residual. In general the 2D IMF1 frequency is higher than that of any other 2D IMF within the same segment. The iris image is decomposed with the DEMD method described above. In this work, an original iris image decomposed into four 2D IMFs. The image's four 2D IMFs and the last residue using DEMD (θ=0^0) as shown in Fig.4.

3.3.3 Fractal Dimension

Fractal provides a mathematical framework which can be applied to describe self-similarity, and irregularity with fractal dimension. Iris images which include abundant information as freckles, stripes, textures are self-similarity. It can intuitively be thought as irregular geometric representation in human's iris. Thus, the fractal dimension can be used to illustrate an iris image. In the situation of an ideal fractal image, the fractal dimension (FD) can be computed using

$$FD = \log(N_r) / \log(1/r), \quad (5)$$

where r and N_r will be explained in the following. Most of the texture images are not ideal fractal images. Of the wide variety of methods for estimating the fractal dimension that have so far been proposed [43, 44], the differential box-counting (DBC) method is one of the more widely used ones [45], as it can be computed automatically and can be applied to patterns with or without self-similarity.

In the DBC method, an image measuring size $M \times M$ pixels is scaled down to $s \times s$, where $1 < s \le M/2$, and s is an integer. Then $r = s/M$. The image is treated as a three-dimensional space, where two dimensions define the coordinates (x,y) of the pixels and the third coordinate (z) defines their grayscale values. The (x,y) is partitioned into grids measuring $s \times s$. The three-dimensional space is partitioned into boxes of size $s \times s \times s$. The boxes are indexed with (i,j,k) in the (x,y,z) space. If the minimum and the maximum grayscale levels in the (i,j) *th* grid respectively fall into the k th and l th boxes, the contribution of n_r in the (i,j) *th* grid is defined as

$$n_r(i,j) = l - k + 1, \quad (6)$$

In this method, N_r is defined as the summation of the contributions from all the grids that are located in a window of the image

$$N_r = \sum_{i,j} n_r(i,j), \quad (7)$$

If N_r is computed for different values of r (i.e., different sizes of the partitioned boxes), then the fractal dimension can be estimated from the least-square linear fit of $\log(N_r)$ against $\log(1/r)$.

3.3.4 Feature Vector

After the previously mentioned procedures are performed for iris image preprocessing, noise (i.e., eyelashes and eyelids) still exists in a lot of iris images, especially in the *CASIA Iris Database*. We observed that they appear in some of the iris subparts. Daugman's approach [5] performed iris recognition based on small portions of the iris, where noise is less probable. Furthermore, Daugman's new methods [8, 9] use the entire visible iris, excluding only regions obscured by noise. To cope with the noise problem, at first, each iris component image is partitioned into several regions, and the DBC method is applied to estimate the fractal

dimension of each region. The aim is to ensure that some sub-regions are noise-free, and matching with the individually enrolled sub-region can be accurate. As described later in the matching processes (Sec. 3.4), this method contributes to a substantial decrease in the error rates for the recognition of noisy iris images.

In this work, the original iris image was decomposed into four 2D IMFs (2D IMF1, 2D IMF2, 2D IMF3 and 2D IMF4) and residuals $\mathrm{Res}(x,y)$ by DEMD.

$$\mathrm{Ori}(x,y)=\sum_{i=1}^{4}\mathrm{2DIMF}_i(x,y)+\mathrm{Res}(x,y) \qquad (8)$$

where $Ori(x,y)$ are the original 2D iris image, 2D IMF$i(x,y)$ are the 2D IMFs and $\mathrm{Res}(x,y)$ are the 2D residual for zero extrema. Typical component images from a normalized iris image are shown in Fig. 4. For the ROI of each component iris image 2D IMF, we divided the iris image into 64 $[(32/16)\times(512/16)]$ non-overlap regions, as illustrated in Fig. 5. Then the fractal dimension of each sub-region (16×16) is estimated. Putting together all fractal dimensions from the image sub-regions of all component images, we can arrange to form a 1-D feature vector V, represented by

$$V=\left[FD_{1,1},FD_{1,2},...,FD_{1,j},...,FD_{i,1},...,FD_{i,j}\right]. \qquad (9)$$

where *i* is the number of 2D IMF component image, *j* is the sub-region number of each iris component image, and $FD_{i,j}$ is the feature value of fractal dimension. Therefore, we can obtain the 256 (4×64) dimensional feature vector to represent one iris image.

3.4 Iris Matching

The main goal of iris recognition is to match the unknown iris feature with those known iris feature classes in the database and determine whether the unknown feature comes from the authentic one or the impostor. The matching process is to be made with the unknown feature, which will be calculated depending on different metrics. The different similarity measures are used as the matching criterion.

3.4.1. Minkowski Distance measure

The Minkowski distance is a generalized measure that includes other distances. For two vectors $x=[x_1,x_2,...,x_n]$ and $y=[y_1,y_2,...,y_n]$,

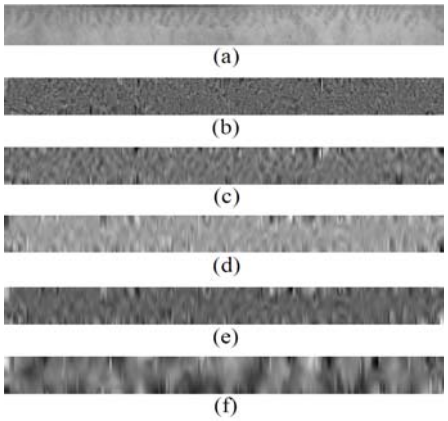

Fig. 4. Multiscale decomposition of an iris image: (a) the original image, (b)~(e) the 2D IMFs from finer to coarser scales and (f) the residue.

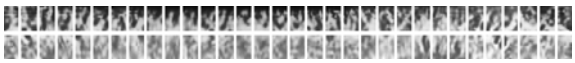

Fig. 5. Dividing the ROI of each component into 64 non-overlap regions.

the Minkowski distance of order p is defined as

$$d_p(x,y)=\left[\sum_{i=1}^{n}(x_i-y_i)^p\right]^{\frac{1}{p}} \qquad (10)$$

Where $p>0$.

The Minkowski distance assumes different names depending on the value of p. If $p=1$, then the distance is called a Manhattan (or city-block) distance. For binary data, the Manhattan distance is called the Hamming distance. The famous Euclidean distance can be computed from equation (10) by selecting $p=2$. The Euclidean distance is one of the simplest and most popular distance measures.

3.4.2. Cosine Distance measure

The Cosine distance is obtained by using the cosine similarity (Orchini similarity, angular similarity, normalized dot product), which measures similarity between two vectors by finding their angle. Cosine distance is calculated by the following formula:

$$d_\alpha(x,y) = 1 - \left(\frac{x \bullet y}{\|x\|\|y\|} \right) \quad (11)$$

where x and y are two different feature vector. $x \bullet y = \sum_{i=1}^{n} x_i y_i$ and $\|x\| = \sqrt{\sum_{i=1}^{n} x_i^2}$. The range of $\frac{x \bullet y}{\|x\|\|y\|}$ is $[0,1]$. The more similar the two vectors are, the smaller the $d_\alpha(x,y)$ value is.

3.4.3. Kullback-Leibler (K-L) Distance measure

The Kullback-Leibler (K-L) distance is perhaps the most frequently used to evaluate the distance between two sequences of random variables that have the same Markovian dependence order [46] because of its geometrical importance.

$$d_{KL}(x,y) = \sum_{i=1}^{n} x_i \ln(x_i / y_i) \quad (12)$$

IV. EXPERIMENTAL RESULTS

To evaluate the validity of the proposed method for iris recognition, two publicly available iris databases, Institute of Automation, Chinese Academy of Science (CASIA) [47] and ICE [48] are adopted as the test datasets. The CASIA database mainly comes from Chinese volunteers and the iris images were collected using OKIs hand-held iris sensor. The Iris Challenge Evaluation (ICE) was conducted under the auspices of the National Institute of Standards and Technology (NIST). The experiments are conducted in two modes: identification (one-to-many matching) and verification (one-to-one matching). In the identification mode, for a test iris image, the algorithm performs a one-to-many search among the entire database to find a template similar to the test image. If the test sample and the found template are in the same class, this is some correct recognition. Therefore, in identification mode, the correct recognition rate (CRR) is adopted to evaluate the efficacy of the algorithm. In the verification mode, if a presented iris image comes from a specified subject, one-to-one matching is executed to verify whether the image is from the specified subject or not. Then, the receiver operating characteristic (ROC) curve, which depicts the relationship of false acceptance rate (FAR) versus false reject rate (FRR), is used. The ROC curve is normally used to measure the accuracy of the matching process, showing the achieved performance of an algorithm. FAR is the probability of accepting an impostor as an authorized subject, and FRR is the probability of an actual authorized subject that is rejected as being an impostor. Meanwhile, the equal error rate (EER) is also used for performance evaluation.

4.1 Iris Database

Experimental evaluation of iris recognition system is carried on the iris images collected from the two publicly available iris databases, CASIA (version 3.0) and ICE. The CASIA iris database is a large open iris database and we only use the subset of it for iris recognition. Its images incorporate few types of noises which are almost exclusively related to eyelid and eyelash obstruction. Each image has the resolution of 640×480 in 8-bit gray level. This database includes 8220 iris images of 411 different eyes (hence, 411 different classes) with 20 images captured for each class. The ICE 2005 database, used in recent Iris Challenge Evaluation contains iris images from 244 different eyes. The total number of images present in the database is 2953. Its main characteristic is the same as that of the CASIA iris database. ICE iris database also incorporates images with several noise factors, thus those images are suitable for evaluating the performance of iris recognition. Each image size has the resolution of 640×480 in TIFF format.

As mentioned above, to evaluate recognition accuracy both in highly and less noisy environments, a large number of images from the CASIA and ICE databases have been selected. Both iris databases contain over 200 classes. The following experiment results will demonstrate the eminent performance of the proposed method. The experiments conducted below executed on the computing environment of 1.8GHz PC with 736MB RAM using Malta 7.0.

4.2 Performance Evaluation of Iris Recognition

Based on Eq. (1), two quality descriptors (q_1 and q_2) of the in focus image and the

Table 1. The number of invalid iris images by quality assessment

Cause of Failure	Number of images	
	CASIA	ICE
(1) Failed iris location (noises within iris)	431	9
(2) Blurred images	85	33
(3)Occlusion by eyelids and eyelash	302	115
Total	818	157

Table 2. Recognition rates achieved by proposed method with three similarity measures

Similarity measures	CASIA database		ICE database	
	FRR (%) at 0.001 FAR (%)	CRR (%)	FRR (%) at 0.001 FAR (%)	CRR (%)
Minkowski distance	0.11	100	0.19	100
Cosine distance	1.21	99.5	0.58	99.8
K-L distance	4.56	98.7	2.39	99.2

useful (un-occluded) image are respectively estimated at the 95% confidence interval in the two iris databases. We can accurately assess the quality of an image and select the iris images of high quality from the input sequence. In Table 1, there are 7402 and 2796 iris images retained for evaluation in the two databases after removing useless iris images. The procedure for finding the quality descriptor of q_2 is involves the iris locating stage, so most of the poor quality images are caused by the iris location failure, especially in the CASIA database. In fact, there are many noisy iris images (caused by eyelid and eyelash occlusion) which can not be located accurately and used for iris recognition. Table 1 also shows the various factors that degrade the iris image quality.

Our experiments on the ICE database show the Minkowski distance measure with outstanding performance among the three similarity measures. Fig. 6 shows the False Acceptance Rate and False Rejection Rate curves, from which it can be seen that when the threshold value for the Minkowski distance measure is 0.25 and the equal error rate (EER) is approximately 0%. Note that performance differences are not very significant while different similarity measures are used. Table 2 demonstrates promising recognition results achieved by our proposed method with three different similarity measures from Eqs. (10)–(12). Only a slightly lower recognition rate of 99.16% is accomplished by using the K-L distance measure in the identification tests in the ICE database. This result supports our decision to use the three similarity measures to recognize the iris patterns.

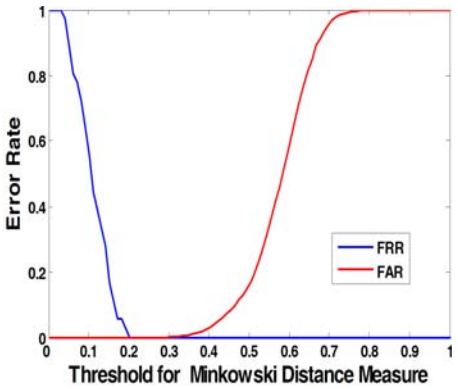

Fig. 6. Error rate curves for minutiae recognition using Minkowski distance measure (EER=0% where the threshold is 0.25)

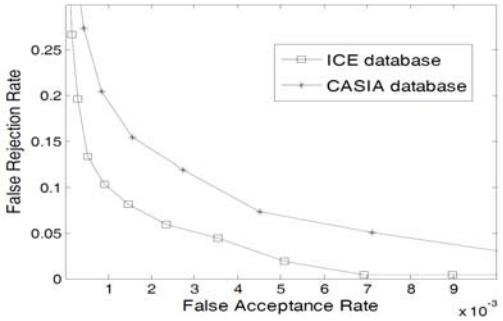

Fig. 7. The ROC curves of two different databases using the Minkowski distance measure.

4.3 Comparison and Discussion

In [24], we use the 1D EMD as a low-pass filter and only the distinct iris characteristics are utilized as discriminating features for accurate iris recognition. Although experimental results show that the 1D EMD is suitable for feature

extraction, it is not to take into account the 2D spatial correlation of the iris image. In this work, we proposed the algorithm of iris recognition based on the DEMD and FD methods. DEMD can separate the normalized iris image into a small set of 2D IMFs, and each one represent 2D iris image of different frequency. Our results

Table 3 Recognition rates achieved by different methods on the ICE database

Methods	CRR (%)	EER (%)
Daugman [6]	100	0.19
Ma *et al.* [25]	99.59	0.39
Previous(LEP)[23]	99.53	0.48
Previous(EMD)[24]	97.22	1.82
Proposed method	100	0.24

showed good recognition rate, as we have considered different frequency features from the normalized iris image. Calculation of fractal dimensions will be quite unlike if we consider the 2D IMFs of different frequency. Also to reduce the time complexity we have considered the 2D IMF1, 2D IMF2, 2D IMF3 and 2D IMF4 only. The 2D IMF1~2D IMF4 decrease in frequency, but the frequency of 2D IMFi is higher than that of 2D IMFi+1. A benefit of directional Empirical Mode Decomposition is their high conjoint resolution, which means that their response (mode) is highly localized in both space and spatial frequency and is adaptive concerning the global information. Experimental results demonstrated in Table 3 reveal that the DEMD technique is an effective scheme for iris recognition than the 1D EMD. Experimental results demonstrated in Sec. 4.2 reveal that the proposed method is an effective scheme for feature extraction from iris images and the similarity measure method of Minkowski distance can achieve a correct recognition rate up to 100% for the two iris databases (CASIA and ICE). The approaches of the 2-D Gabor filters [5], and the Gaussian-Hermite moments [10] are well-known ones among the existing schemes for iris recognition. Here, we also use the previous works with LEP and EMD methods [23, 24] to extract the iris feature for iris recognition to compare with the proposed method. To compare the proposed technique with those schemes, the results are shown in Table 3 after implementing those iris recognition algorithms. Together with our proposed scheme, five approaches are tested using the 244 classes of the ICE iris database. As shown in Table 3 and Fig. 8, the proposed method still can fulfill the demand of high accuracy suitable for very high security environments. Figure 8 displays the ROC curve of those five methods. Experimental results demonstrate that our method is much better than the two methods of previous work [23, 24], and can compete with

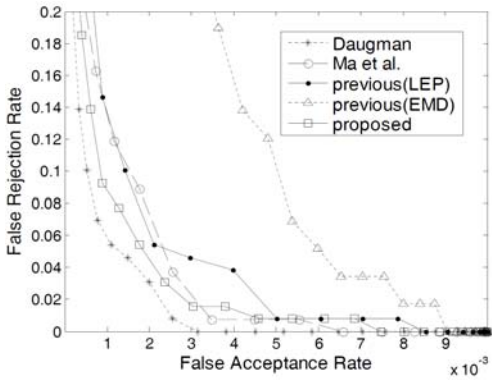

Fig. 8. ROC plot depicts the performance of the different algorithms on the ICE iris database

Table 4 Average time of the proposed method for the steps

Methods	Time (ms)
Iris quality assessment	1218
Iris image preprocessing	526
Feature extraction	397
Feature matching	34
Total execution time	2175

the other two approaches, Daugman [5] and Ma et al. [10]. The total time for identifying one iris images from database is average 2.17 second on the same hardware (described in Sec. 4.1). Table 4 shows the computation time with the execution time in average for iris image quality assessment, image preprocessing, feature extraction and matching.The accomplished ROC curves to the two databases of CASIA and ICE are shown in Fig. 7. Notably, the recognition performance by applying the proposed method to the ICE iris database is better than that of the CASIA iris database. The main reason is that the iris texture information about Asian subjects is less discriminative than that of the Western, especially on the regions far from the pupil. As observed in Table 2, the proposed algorithm exhibiting the recognition performance is very high and the FRR is very low. Therefore, experimental results demonstrate that the proposed iris representation is effective and the proposed approach can really extract promising

features from each iris image to achieve robustness for iris recognition.

V. CONCLUSION

Automatic iris recognition has been studied for more than a decade. In [24], we used the 1-D empirical mode decomposition (EMD) as a low-pass filter to extract the iris features for accurate iris recognition, but it does not take into account the 2D correlation of image. In addition, there is no general method finding the direction of iris texture, although it is very important in iris recognition. According to the texture analysis of the iris images, a new method of feature extraction for iris recognition is presented, which operates using the DEMD and fractal dimension technique. The DEMD method is applied to decompose iris image into a small set of sub-images called 2D IMFs representing the different frequencies (scales) of the iris image. Fractal dimensions obtained from multiple scale features are used to characterize the iris textures completely. The experimental results with two publicly available iris image databases, CASIA and ICE, illustrate the effectiveness of the proposed method. The performance of iris recognition achieved by the proposed approach associated with three different similarity measures is evaluated. The best similarity metric is the Minkowski distance measure, and the other two similarity measures also achieve similar performance of more than 99%. The proposed algorithms are also compared with existing algorithms and the performance is highly suitable for real time applications. Therefore, we propose a novel and efficient method for personal identification with iris images.

REFERENCES

[1] Jain, A K, Ross A, and Prabhakar, S, “An introduction to biometric recognition,” IEEE transactions on circuits and systems for video technology—special issue on image and video-based biometrics, Vol.14, No.1, January, 2004.

[2] Kashima, H, Hongo, H, Kato, K, and Yamamoto, K, “A robust iris detection method of facial and eye movement,” Canadian conference on computer and robot vision (CRV), 2001.

[3] Jain, A. K., Bolle, R., and Pankanti, S., Biometrics: Personal Identification in Network Society, Kluwer Academic Publishers, 1999.

[4] Miller, B., “Vital Signs of Identity,” IEEE Spectrum, Vol. 31, pp. 22-30, 1994.

[5] Daugman, J., “High confidence visual recognition of persons by a test of statistical independence,” IEEE Trans. Pattern Anal. Mach. Intell., Vol.15, No.11, pp. 1148–1161, 1993.

[6] Daugman, J., “Statistical richness of visual phase information: update on recognizing persons by iris patterns,” Int. J. Comput. Vis. Vol. 45, No. 1, pp. 25–38, 2001.

[7]. Daugman, J., “How iris recognition works,” IEEE Trans. Circuits Syst. Video Technol. Vol. 14, No. 1, pp. 21–30, 2004.

[8] Daugman, J., “Probing the uniqueness and randomness of iriscodes: Results from 200 billioniris pair comparisons,” Proc. IEEE, Vol. 94, No. 11, pp. 1927–1935, 2006.

[9]. Daugman, J., “New methods in iris recognition,” IEEE Trans. Syst., Man, Cybern., Part B: Cybern. Vol. 37, No. 5, pp. 1167–1175, 2007.

[10] Ma, L., Tan, T., Wang, Y., and Zhang, D., “Local intensity variation analysis for iris recognition,” Pattern Recogn. Vol. 37, pp. 1287–1298, 2004.

[11] Wildes, R., “Iris recognition: an emerging biometric technology,” Proc. IEEE, Vol. 85, No. 9, pp. 1348–1363, 1997.

[12] Huang, N., Shen, Z., Long, S., Wu, M., Shih, H., Zheng, Q., Yen, N., Tung,. C., and Liu, H., “The empirical mode decomposition, and Hilbert spectrum for nonlinear and non-stationary time series analysis,” Proc.R. Soc. London, Vol. 454, pp.903–995, 1998.

[13] Huang, N. E. and Wu, M. L., “Application of Hilbert-Huang transform to non-stationary financial time series analysis”, Appl. Stochastic Models Bus.Ind, Vol. 19, No. 6, pp. 245–268, 2003.

[14] Zhang, R. R. et al, “Hilbert-Huang Transform analysis of dynamic and earthquake motion recordings”, Journal of Engineering Mechanics, Vol. 8,pp. 861–875, 2003.

[15] Liu, Z. X. and Peng, S. L.,. "Directional EMD and its application to texture segmentation," China Ser. F, Inf., Vol. 48, No. 3, pp. 354–365, 2005.
[16] Boles, W. W. and Boashash, B., "A human identification technique using images of the iris and wavelet transform," IEEE Trans. Signal Process. Vol. 46, No. 4, pp. 1185–1188, 1998.
[17] Sanchez-Avila, C. and Sanchez-Reillo, R., "Iris-based biometric recognition using dyadic wavelet transform," IEEE Aerosp. Electron. Syst. Mag. Vol. 17, No. 1, pp. 3–6, 2002.
[18] Monro, D., Rakshit, S., and Zhang, D., "DCT-based iris recognition," IEEE Trans. Pattern Anal. Mach. Intell. Vol. 29, No. 4, pp. 586–595, 2007.
[19] Wildes, R., Asmuth, J., Green, G., Hsu, S., Kolczynski, R., Matey, J., and McBride, S., "A machine-vision system for iris recognition," Mach.Vision Appl. Vol. 9, No. 1, pp. 1–8, 1996.
[20] Lim, S., Lee K., Byeon, O., and Kim, T., "Efficient iris recognition through improvement of feature vector and classifier," ETRI J. Vol. 23, No. 2, pp 61–70, 2001.
[21] Ma, L., Tan, T., Wang, Y., and Zhang, D., "Personal identification based on iris texture analysis," IEEE Trans. Pattern Anal. Mach. Intell. Vol. 25, No. 12, pp. 1519–1533, 2003.
[22] Tisse, C., Martin, L., Torres, L., and Robert, M., "Person identification technique using human iris recognition," J. Syst. Res. Vol. 4, pp. 67–75, 2003.
[23] Lee, J. C., Huang, P. S., Chang, J. C., Chang, C. P., and Tu, T. M., "Iris recognition using local texture analysis," Opt. Eng. Vol. 47, No. 6, pp. 067205-1–67205-10, 2008.
[24] Chang, C. P., Lee, J. C., Su, Y., Huang, P. S., and Tu, T. M., "Using Empirical Mode Decomposition for Iris Recognition," Computer Standards & Interfaces, Vol. 31, pp. 729-739, 2009.
[25] Ma, L., Tan, T., Wang, Y., and Zhang, D., "Efficient iris recognition by characterizing key local variations," IEEE Trans. Image Process., Vol. 13, No. 6, pp. 739–750, 2004.
[26] Noh, S. I., Bae, K., Park, K. R., and Kim, J., "A new iris recognition method using independent component analysis," IEICE Transactions on Information and Systems, Vol. E88-D, pp. 2573-2581, 2005.
[27] Proença, H. and Alexandre, L. A., "Toward non-cooperative Iris recognition: A classification approach using multiple signatures," IEEE Transactions on Pattern Analysis and Machine Intelligence, Vol. 29, pp. 607-612, 2007.
[28] Daubechies, I., Ten Lectures on Wavelets, SIAM, Philadelphia, PA, 1992.
[29] Wang, S. S., Chen, P. C., and Lin, W. G., "Invariant pattern recognition by moment Fourier descriptor," Pattern Recogn., Vol. 27, pp. 1735–1742, 1994.
[30] Granlund, G. H., "Fourier processing for handwritten character recognition," IEEE Trans. Comput., Vol. 21, pp. 195–201, 1992.
[31] Wunsch, P. and Laine, A. F., "Wavelet descriptors for multiresolution recognition of handprinted characters," Pattern Recogn., Vol. 28, pp. 1237–1249, 1995.
[32] Mandelbrot, B. B., Van Ness, J. W., "Fractional Brownian motions, fractional noises and applications", SIAM Review, Vol. 10, pp. 422-437, 1968.
[33] Charlampidi, D. and Kasparis, T., "Rotationally invariant texture segmentation using directional wavelet-based fractal dimensions", Proc. SPIE, Vol. 4391, pp.115-126, 2001.
[34] Asvestas, P., Matsopoulos, G. K., and Nikita, K. S., "Estimation of fractal dimension of images using a fixed mass approach," Pattern Recognition Letters, Vol. 20, pp. 347-354, 1999.
[35] Jin, X. C. and Jayasooriah, O. S. H., "A practical method for estimating fractal dimension," Pattern Recognition Letters, Vol. 16, pp. 457-464, 1995.
[36] Sarkar, N. and Chaudhuri, B. B., "An efficient approach to estimate fractal dimension of textured images," Pattern Recognition, Vol. 25, pp. 1035-1041, 1992.
[37] Chen, W. S. and Yuan, S. Y., "A novel personal biometric authentication technique using human iris based on fractal dimension features," in Proceedings of the International Conference on Acoustics, Speech and Signal Processing, Vol. 3, pp. 201-204, 2003.

[38] Tsai, C. C., Taur, J. S., and Tao, C. W., "Iris Recognition Using Gabor Filters and the Fractal Dimension ," Journal of Information Science and Engineering, Vol. 25, No. 2, pp. 633-648, 2009.
[39] Lee, J. C., Su, Y., Tu, T. M., and Chang, C. P.," A Novel Approach to Image Assessment in Iris Recognition System," Imaging Science Journal, Vol. 58, No. 3, pp. 136-145, 2010.
[40] Sung, H., Lim, J., Park, J., and Lee, Y., "Iris recognition using collarette boundary localization," Proc. 17th Intl. Conf. Patt. Recog., Vol. 4, pp. 857–860, 2004.
[41] Rilling, G., Flandrin, P., and Goncalves, P., "Empirical mode decomposition as a filter bank," IEEE Signal Process, Vol. 11, No. 2, pp. 112–114, 2004.
[42] Flandrin, P., Gonçalvés, P., and Rilling, G., "Detrending and denoising with empirical mode decomposition," Proc. 12th European Signal Processing Conf., pp. 1581–1584, 2004.
[43] Chaudhuri,, B. B.and Sarkar, N., "Texture Segmentation using fractal dimension," IEEE Trans. Pattern Anal. Mach. Intell., Vol. 17, No. 1, pp. 72–77, 1995.
[44] Peitgen, H. O., Jurgens, H., and Saupe, D., "Chaos and Fractals: New Frontiers of Science," Springer, Berlin, pp. 202–213, 1992.
[45] Peitgen, H. O., Jurgens, H., and Saupe, D., Chaos and Fractals New Frontiers of Science, Springer, New York, 1992.
[46] Kullback, S., Information theory and statistics, Dover, 1968.
[47] Institute of Automation, Chinese Academy of Science. CASIA Iris Image Database, http://www.sinobiometrics.com/chinese/chinese.htm
[48] National Institute of Science and Technology. Iris Challenge Evaluation, http://iris.nist.gov/ICE, 2005.